Polymer Chemistry

Accepted Manuscript

ROYAL SOCIETY OF CHEMISTRY

www.rsc.org/polymers

Cite this: DOI: 10.1039/c0xx00000x

www.rsc.org/xxxxxx

ARTICLE TYPE

In situ synthesis of thermo-responsive ABC triblock terpolymer nano-objects by seeded RAFT polymerization

Yaqing Qu, Fei Huo, Quanlong Li, Xin He, Shentong Li, and Wangqing Zhang*

Received (in XXX, XXX) Xth XXXXXXXXX 20XX, Accepted Xth XXXXXXXXX 20XX

DOI: 10.1039/b000000x

Abstract. RAFT polymerization of *N*-isopropylacrylamide under heterogeneous condition in the presence of the diblock copolymer nano-objects of polystyrene-*block*-poly(*N*,*N*-dimethylacrylamide) trithiocarbonate (PS-*b*-PDMA-TTC) with the *Z*-group RAFT terminal at the outer side of the solvophilic poly(*N*,*N*-dimethylacrylamide) (PDMA) block is performed. This heterogeneous RAFT polymerization, which is named seeded RAFT polymerization, affords the in situ synthesis of the polystyrene-*block*-poly(*N*,*N*-dimethylacrylamide)-*block*-poly(*N*-isopropylacrylamide) (PS-*b*-PDMA-*b*-PNIPAM) triblock terpolymer nano-objects. The molecular weight of the triblock terpolymer linearly increases with the monomer conversion during the seeded RAFT polymerization. The morphology of the PS-*b*-PDMA-*b*-PNIPAM triblock terpolymer nano-objects is justly duplicated from the seed of the PS-*b*-PDMA-TTC diblock copolymer, which are the binary mixture of nanospheres and nanorods, when the polymerization degree (DP) of the poly(*N*-isopropylacrylamide) (PNIPAM) block is low or moderately large. When the DP of the PNIPAM block is relatively large, the triblock terpolymer nanospheres are formed. The size of the PS-*b*-PDMA-*b*-PNIPAM triblock terpolymer nano-objects slightly increases initially and subsequently decreases with the monomer conversion during the seeded RAFT polymerization. In water at temperature above the phase-transition temperature (PTT) of the PNIPAM block, the PNIPAM chains deposit onto the polystyrene (PS) core to form the triblock terpolymer multicompartment nano-objects containing a microphase separated solvophobic core of PS/PNIPAM and a solvophilic PDMA corona. Our findings are anticipated to be useful in preparation of concentrated ABC triblock terpolymer nano-objects.

1 Introduction

ABC triblock terpolymer nano-objects, especially amphiphilic ABC triblock terpolymer nano-objects, have aroused great interest because of their complex structures compared with those of AB diblock copolymers.[1] The amphiphilic triblock terpolymer nano-objects are usually prepared through the micellization of ABC triblock terpolymer in the selective solvent for the A, B, or/and C block.[2-24] Dependent on the triblock terpolymer structure such as the block length,[2,3] the block order (ABC, ACB, and CAB),[4-6] and the solvophilic/solvophobic ratio,[7] the solvent character,[8] and even the process of micellization,[9] various nano-objects such as core-corona nanospheres,[10,11] core-shell-corona nanospheres,[12-14] multicompartment nanoparticles,[2-5] nanorods,[15-17] and vesicles[18,19] have been prepared. Of all these ABC triblock terpolymer nano-objects, those containing a thermo-responsive block are especially interesting,[20-24] since this thermo-responsive block endows the ABC triblock terpolymer nano-objects with additional response to the thermal stimulus at the lower critical solution temperature (LCST)[20-22] or the upper critical solution temperature (UCST).[23,24] Compared with the thermo-responsive AB diblock copolymer nano-objects,[25-29] the examples of thermo-responsive ABC triblock terpolymer nano-objects are relatively scarce,[20-24] and two possible reasons are ascribed to the scarcity. First, synthesis of a well-controlled thermo-responsive ABC triblock terpolymer is a laborious work, even by the relatively convenient technique of the controlled radical polymerization including atom transfer radical polymerization (ATRP),[30,31] nitroxide-mediated polymerization (NMP),[32] and reversible addition-fragmentation chain transfer (RAFT) polymerization.[33,34] Second, the micellization strategy suffers from the drawbacks of the dilute block copolymer concentration (usually below 1 wt%) and the time-consuming multiple steps,[2-24] which make the preparation of ABC triblock terpolymer nano-objects somewhat irreproducible.

Recently, we proposed a heterogeneous RAFT polymerization named seeded RAFT polymerization to in situ synthesize ABA or ABC triblock copolymer nano-objects in the alcoholic solvent.[35-37] This seeded RAFT polymerization to prepare triblock copolymer nano-objects has three characters. First, uniform diblock copolymer nanoparticles containing suitable RAFT terminal instead of soluble small RAFT agent or soluble macromolecular RAFT (macro-RAFT) agent are employed, which makes the RAFT polymerization under full-stage heterogeneous condition and therefore to accelerate the RAFT polymerization. Second, the in situ preparation of triblock terpolymer nano-objects is achieved, and the size and morphology of the triblock terpolymer nano-objects change with the monomer conversion during the seeded RAFT polymerization. Third, the concentration of the triblock terpolymer nano-objects is relatively high, *e.g.* 20 wt%, which is much beyond the micellization regime and is proportional to the polymerization-induced self-assembly proposed by Charleux and coworkers.[38]

In this contribution, we extend this seeded RAFT polymerization to synthesize thermo-responsive ABC triblock terpolymer nano-objects of polystyrene-*block*-poly(*N*,*N*-dimethylacrylamide)-*block*-poly(*N*-isopropylacrylamide) (PS-*b*-PDMA-*b*-PNIPAM). Results demonstrated that well-defined PS-

b-PDMA-*b*-PNIPAM nanospheres and nanorods are prepared in the alcoholic solvent. In water at temperature below the phase-transition temperature (PTT) of the poly(*N*-isopropylacrylamide) (PNIPAM) block, the PS-*b*-PDMA-*b*-PNIPAM nanospheres have core-corona structure, in which the solvophobic block of polystyrene (PS) forms the core and the solvophilic diblock of poly(*N*,*N*-dimethylacrylamide)-*block*-poly(*N*-isopropylacrylamide) forms the corona. At temperature above PTT, the PNIPAM block deposits onto the PS core to form ABC triblock terpolymer multicompartment nanoparticles.

2 Experimental Section

2.1 Materials

The monomer of *N*-isopropylacrylamide (NIPAM, >99%, Acros Organics) was purified by recrystallization in the acetone/*n*-hexane mixture (50/50 by volume). The monomer of *N*,*N*-dimethylacrylamide (DMA, 99.5%, Alfa) and styrene (St, >98%, Tianjin Chemical Company) were distilled under reduced pressure and stored at -5 ^{o}C prior to use. The RAFT agent of 4-cyano-4-(ethylsulfanylthiocarbonyl) sulfanylpentanoic acid (ECT, Scheme S1) was synthesized as discussed elsewhere.[39] The initiator of 2,2'-azobis(2-methylpropionitrile) (AIBN, >99%, Tianjin Chemical Company) was purified by recrystallization from ethanol. Other chemical reagents were analytic grade and used as received. Deionized water was used in the present experiments.

2.2 Synthesis of the PS-*b*-PDMA-TTC diblock copolymer

The diblock copolymer of PS-*b*-PDMA-TTC was synthesized by sequential solution RAFT polymerization using AIBN as initiator as discussed elsewhere.[40] Typically, into a 100 mL Schlenk flask with a magnetic bar, St (30.0 g, 0.288 mol), ECT (0.252 g, 0.958 mmol), and AIBN (53.4 mg, 0.325 mmol) dissolved in 1,4-dioxane (18.0 g) were added. The solution was initially degassed with nitrogen at 0 ^{o}C for 30 min, and then the flask content was immersed into a preheated oil bath at 70 ^{o}C for 18 h. The polymerization was quenched by rapid cooling upon immersion of the flask in iced water. The monomer conversion at 45.1% was determined by ^{1}H NMR analysis in the presence of the internal standard of 1,3,5-trioxane. The synthesized polymer was precipitated into ethanol, collected by three precipitation/filtration cycles, and then dried at room temperature under vacuum to afford the PS-TTC macro-RAFT agent. Subsequently, into a 50 mL Schlenk flask with a magnetic bar, the synthesized PS-TTC (12.0 g, 0.836 mmol), DMA (6.63 g, 66.9 mmol), and AIBN (45.7 mg, 0.278 mmol) dissolved in 1,4-dioxane (8.00 g) were added. The solution was initially degassed with nitrogen at 0 ^{o}C for 30 min, and then the polymerization was performed at 70 ^{o}C for 4 h. The polymerization was quenched by rapid cooling upon immersion of the flask into iced water. The monomer conversion at 100% was determined by ^{1}H NMR analysis in the presence of the internal standard of 1,3,5-trioxane. The synthesized polymer was precipitated into the mixture of diethyl ether and *n*-hexane (3:1 by weight), collected by three precipitation/filtration cycles, washed twice with ethanol, and lastly dried at room temperature under vacuum to afford the PS-*b*-PDMA-TTC diblock copolymer.

2.3 Preparation of the PS-*b*-PDMA-TTC seed-nanoparticles

Into a 25 mL Schlenk flask with a magnetic bar, the synthesized PS-*b*-PDMA-TTC diblock copolymer (0.246 g, 0.011 mmol) and ethanol (2.40 g) were added, and then the mixture was immersed into an ultrasonic bath (KQ-200KDE, 40 kHz, 200 W, Zhoushan, China) for 20 min at 50 ^{o}C to get a well-dispersed colloidal dispersion. Subsequently, the mixture was cooled to room temperature (~15 ^{o}C), and then the monomer of NIPAM (0.500 g, 4.42 mmol) and water (0.600 g) were added, and lastly the mixture was stirred vigorously for 30 min to afford a bluish dispersion of the PS-*b*-PDMA-TTC seed-nanoparticles. To avoid possible side-reactions, the newly-prepared dispersion of the PS-*b*-PDMA-TTC seed-nanoparticles was used in the subsequent seeded RAFT polymerization.

2.4 Seeded RAFT polymerization and synthesis of the PS-*b*-PDMA-*b*-PNIPAM triblock terpolymer nano-objects

The PS-*b*-PDMA-*b*-PNIPAM triblock terpolymer nano-objects were prepared by seeded RAFT polymerization of NIPAM in the 80/20 ethanol/water mixture under $[NIPAM]_0$:$[PS\text{-}b\text{-}PDMA\text{-}TTC]_0$:$[AIBN]_0$ = 1200:3:1 and with a constant solid concentration at 15 wt%. Into the freshly prepared dispersion of the PS-*b*-PDMA-TTC seed-nanoparticles (0.250 g, 0.011 mmol) containing a given weight of the NIPAM monomer (0.500 g, 4.42 mmol) and the ethanol/water mixture (3.00 g, 80/20 by weight), the initiator of AIBN (0.600 mg, 0.0036 mmol) dissolved in the ethanol/water mixture (1.23 g, 80/20 by weight) was added. The flask content was degassed at 0 ^{o}C for 30 min under vigorous stirring, and then the polymerization was started by immersing the flask into preheated oil bath at 70 ^{o}C. After a given time, the polymerization was quenched by immersing the flask in iced water. The monomer conversion in the seeded RAFT polymerization was detected by ^{1}H NMR analysis. The monomer conversion of NIPAM was calculated according to eqn 1, in which $I_{4.02}$ is the integral area of the proton resonance signals at δ = 4.02 ppm (CONHC***H***$(CH_3)_2$) corresponding to the PNIPAM block in the synthesized polymer, and $I_{4.17}$ is the integral area of the proton resonance signals at δ = 4.17 ppm (CONHC***H***$(CH_3)_2$) corresponding to the remaining NIPAM monomer, respectively.

$$\text{Conversion}\,\% = \frac{I_{4.02}}{I_{4.02} + I_{4.17}} \times 100\,\% \qquad (1)$$

To detect the morphology of the synthesized PS-*b*-PDMA-*b*-PNIPAM triblock terpolymer nano-objects, part of the in situ synthesized triblock terpolymer nano-objects dispersed in the polymerization medium of the 80/20 ethanol/water mixture were dialyzed against water at room temperature, diluted with suitable amount of water, and lastly the morphology of the triblock terpolymer nano-objects at a given temperature was observed by transmission electron microscope (TEM). To check the thermo-response of the PS-*b*-PDMA-*b*-PNIPAM nano-objects, the transmittance of the aqueous dispersion of the triblock terpolymer nano-objects at a given temperature was checked by UV-vis analysis at 500 nm with the heating rate at 1 ^{o}C/min, and PTT was determined at the middle point of the transmittance change.

To collect the PS-*b*-PDMA-*b*-PNIPAM triblock terpolymer for ^{1}H NMR analysis, differential scanning calorimetric (DSC) analysis and gel permeation chromatography (GPC) analysis, part of the in situ synthesized PS-*b*-PDMA-*b*-PNIPAM triblock

terpolymer nano-objects were precipitated into cold diethyl ether, collected by three precipitation/filtration cycles, and then dried at room temperature under vacuum to afford the PS-*b*-PDMA-*b*-PNIPAM triblock terpolymer.

2.5 Apparatus and characterization

The ^{1}H NMR analysis was performed on a Bruker Avance III 400 MHz NMR spectrometer using $CDCl_3$ as solvent. The molecular weight and molecular weight distribution or the polydispersity index (PDI, PDI = M_w/M_n) of the synthesized polymers were determined by a Waters 600E GPC system equipped with three Waters columns of Styragel HT 3, 4 and 5 and a Waters 2414 refractive index detector, where THF was used as eluent at flow rate of 1.0 mL/min at 35.0 °C and the narrow-polydispersity polystyrene (molecular weight: 3370-2060000 Da) was used as calibration standard. TEM observation was performed using a Tecnai G^2 F20 electron microscope at an acceleration of 200 kV. The UV-vis analysis was performed on a Varian 100 UV-vis spectrophotometer. The DSC analysis was performed on a NETZSCH DSC differential scanning calorimeter under nitrogen atmosphere, in which the sample was heated to 200 °C at the heating rate of 10 °C/min, cooled to 0 °C at the cooling rate of 10 °C/min, and then heated to 200 °C at the heating rate of 10 °C/min.

3 Results and discussion

3.1 Synthesis of the PS-*b*-PDMA-TTC diblock copolymer

Scheme 1 shows the synthesis of the PS-*b*-PDMA-TTC diblock copolymer, in which the initial RAFT synthesis of the PS-TTC macro-RAFT agent and the subsequent RAFT polymerization of DMA in the presence of the PS-TTC macro-RAFT agent are included. The RAFT polymerization of styrene under $[St]_0$:$[ECT]_0$[AIBN]$_0$ = 900:3:1 was quenched at moderate monomer conversion of 45.1% to ensure the narrowly-dispersed molecular weight of the synthesized PS-TTC macro-RAFT agent. The theoretical number-average molecular weight ($M_{n,th}$) of the synthesized PS-TTC is 14.3 kg/mol corresponding to the polymerization degree (DP) at 135, in which $M_{n,th}$ is calculated following eqn 2 as described elsewhere.[41] The PS-TTC macro-RAFT agent was characterized by GPC analysis (Figure 1) and ^{1}H NMR analysis (Figure 2). The THF-based GPC analysis gives the polymer molecular weight $M_{n,GPC}$ = 9.7 kg/mol and PDI = 1.22. Based on the characteristic chemical shift at δ = 0.88 ppm ascribed to the RAFT terminal originating from ECT and the chemical shift at δ = 7.22-6.26 ppm ascribed to the phenyl group of the PS-TTC backbone, the PS-TTC molecular weight $M_{n,NMR}$ at 12.7 kg/mol is calculated. It is found that the PS-TTC molecular weight $M_{n,NMR}$ by ^{1}H NMR analysis and $M_{n,th}$ by the monomer conversion are higher than those of $M_{n,GPC}$ by GPC analysis.

$$M_{n,th} = \frac{[\text{monomer}]_0 \times M_{\text{monomer}}}{[\text{RAFT}]_0} \times conversion + M_{\text{RAFT}} \quad (2)$$

The diblock copolymer of PS_{135}-*b*-PDMA-TTC is synthesized by the PS_{135}-TTC macro-RAFT agent mediated polymerization of DMA under $[DMA]_0$:$[PS_{135}\text{-TTC}]_0$:$[AIBN]_0$ = 240:3:1. The RAFT polymerization of DMA runs quickly and almost 100% monomer conversion was achieved in 4 h. Based on this monomer conversion, the theoretical molecular weight $M_{n,th}$ of the synthesized PS_{135}-*b*-PDMA-TTC, 22.3 kg/mol corresponding to the DP of DMA at 80, is calculated. Figure 1 shows the monomodal GPC traces of the synthesized PS_{135}-*b*-PDMA-TTC, and the GPC analysis gives $M_{n,GPC}$ = 14.8 kg/mol and PDI = 1.19. The ^{1}H NMR spectra of PS_{135}-*b*-PDMA-TTC are shown in Figure 2, from which the characteristic chemical shifts due to the PDMA block are clearly observed. Based on the characteristic chemical shift of the PDMA block at δ = 2.90 ppm and that in the phenyl group of the PS block at δ = 7.22-6.26 ppm, the molecular weight $M_{n,NMR}$ at 20.0 kg/mol of the PS_{135}-*b*-PDMA-TTC diblock copolymer is calculated. It is found that the molecular weight $M_{n,th}$ of the PS_{135}-*b*-PDMA-TTC diblock copolymer calculated by the monomer conversion and $M_{n,NMR}$ by ^{1}H NMR analysis are higher than those of $M_{n,GPC}$ by GPC analysis. The underestimated molecular weight $M_{n,GPC}$ is possibly ascribed to adsorption of the Nitrogen-containing polymer onto the GPC columns during the GPC analysis. In the later discussion, the synthesized diblock copolymer is labeled as PS_{135}-*b*-$PDMA_{80}$-TTC, in which the subscripts represent the DP of the corresponding blocks calculated by the monomer conversion.

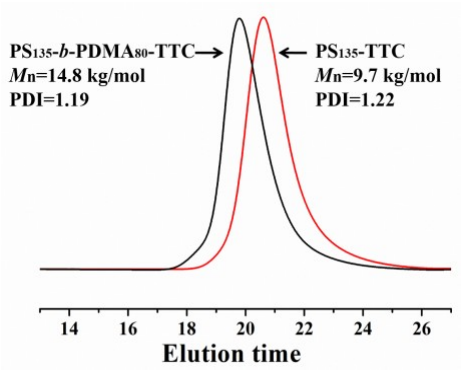

Figure 1. The GPC traces of the PS_{135}-TTC macro-RAFT agent and the PS_{135}-*b*-$PDMA_{80}$-TTC diblock copolymer.

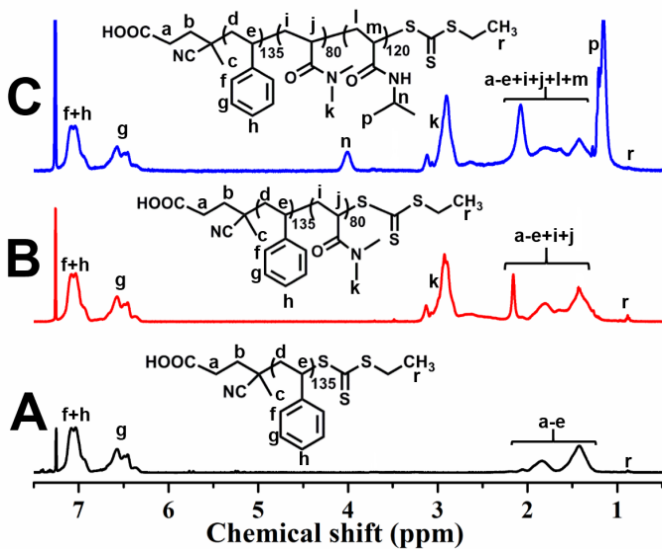

Figure 2. ^{1}H NMR spectra of PS_{135}-TTC (A), PS_{135}-*b*-$PDMA_{80}$-TTC (B), and the typical PS_{135}-*b*-$PDMA_{80}$-*b*-$PNIPAM_{120}$ triblock terpolymer (C).

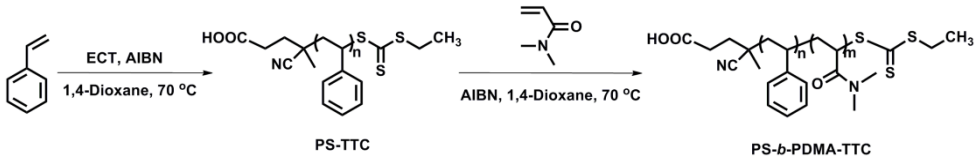

Scheme 1. Synthesis of the PS-*b*-PDMA-TTC diblock copolymer.

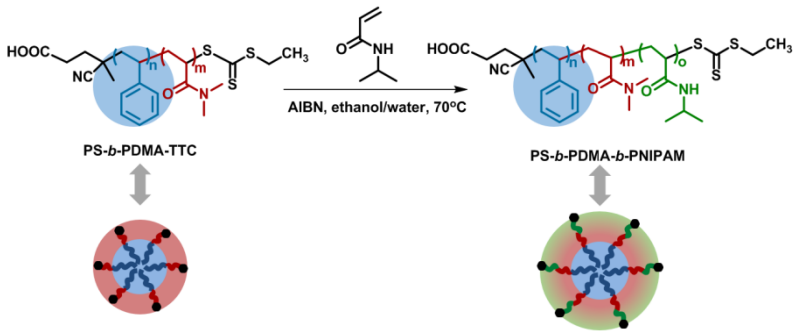

Scheme 2. Seeded RAFT polymerization of *N*-isopropylacrylamide to synthesize the PS-*b*-PDMA-*b*-PNIPAM triblock terpolymer nanoparticles.

3.2 Preparation of the PS-*b*-PDMA-TTC seed-nanoparticles

To be used in the seeded RAFT polymerization to prepare the PS-*b*-PDMA-*b*-PNIPAM triblock terpolymer nano-objects, the dispersion of the seed-nanoparticles with enough high concentration of the PS_{135}-*b*-$PDMA_{80}$-TTC diblock copolymer should be prepared. To achieve this goal, the PS_{135}-*b*-$PDMA_{80}$-TTC diblock copolymer was firstly added in the preheated ethanol at 50 °C, and then dispersed by ultrasonic. Due to the relatively high solvophilic/solvophobic ratio of PS_{135}-*b*-$PDMA_{80}$-TTC and the relatively high temperature, optically uniform colloidal dispersion of the PS_{135}-*b*-$PDMA_{80}$-TTC diblock copolymer with polymer concentration up to 7 wt% can be prepared. The diblock copolymer dispersion was cooled to room temperature (~15 °C), and then suitable amount of the NIPAM monomer and water were added to afford the PS_{135}-*b*-$PDMA_{80}$-TTC seed-nanoparticles dispersed in the ethanol/water/NIPAM (80/20/16.7 by weight) ternary mixture with polymer concentration at 4.9 wt%.

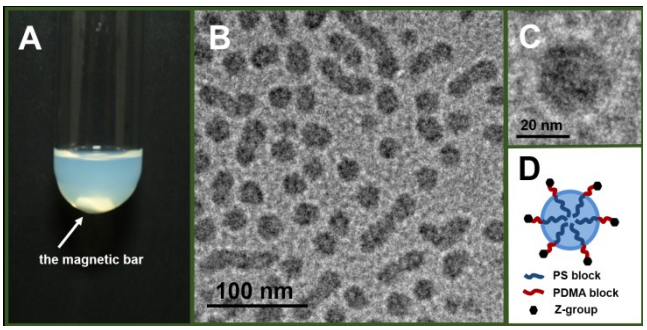

Figure 3. The dispersion of the 4.9 wt% PS_{135}-*b*-$PDMA_{80}$-TTC seed-nanoparticles in the ethanol/water/NIPAM ternary mixture (80/20/16.7 by weight) (A), and the TEM images (B and C) and the schematic structure (D) of the PS_{135}-*b*-$PDMA_{80}$-TTC seed-nanoparticles.

Figure 3A shows the bluish dispersion of the 4.9 wt% seed-nanoparticles of the PS-*b*-PDMA-TTC diblock copolymer, from which the uniform dispersion of the diblock copolymer in the ethanol/water/NIPAM ternary mixture is judged. The TEM images shown in Figures 3B-3C and Figure S1 suggest the coexistence of nanospheres and short nanorods in the bluish dispersion of the PS-*b*-PDMA-TTC seed-nanoparticles. It is found that the diameter of the nanospheres is narrowly centered at 25 nm, and the average diameter is very close to the width of the nanorods as shown in Figure S2, which ensures the similar accessibility of the NIPAM monomer to the seed-nanoparticles during the seeded RAFT polymerization and therefore the narrowly-distributed molecular weight of the PS-*b*-PDMA-*b*-PNIPAM triblock terpolymer. For the sake of briefness, the term of seed-nanoparticles are called in the present study, since nanospheres and nanorods coexist in the PS_{135}-*b*-$PDMA_{80}$-TTC colloidal dispersion. Due to the PS block being insoluble and the PDMA block being soluble in the ethanol/water/NIPAM ternary mixture, the PS-*b*-PDMA-TTC nanospheres should have core-corona structure as shown in Figure 3D, in which the PS block forms the core and the PDMA block containing an outer *Z*-group RAFT terminal forms the corona.

3.3 Seeded RAFT polymerization and in situ synthesis of the triblock terpolymer nano-objects

The seeded RAFT polymerization of NIPAM was performed in the 80/20 ethanol/water mixture in the presence of the PS-*b*-PDMA-TTC seed-nanoparticles under $[NIPAM]_0$:$[PS\text{-}b\text{-}PDMA\text{-}TTC]_0$:$[AIBN]_0$ = 1200:3:1. Since the *Z*-group RAFT terminal is located on the outside of the PDMA block as shown in Figure 3D, the newly-formed PNIPAM block is extended at the outside of the PDMA block to prepare the PS-*b*-PDMA-*b*-PNIPAM triblock terpolymer nano-objects during the seeded RAFT polymerization. Besides, since the monomer of NIPAM and the newly-formed third block of PNIPAM are soluble in the 80/20 ethanol/water mixture, and therefore the seeded RAFT polymerization runs similarly with the homogeneous solution RAFT polymerization. With the progress of the seeded RAFT polymerization, the third solvophilic PNIPAM block extends, and the core-corona seed-nanoparticles of the PS-*b*-PDMA-TTC diblock copolymer containing a PDMA corona convert into core-corona ones containing a PDMA-*b*-PNIPAM diblock corona as shown in Scheme 2.

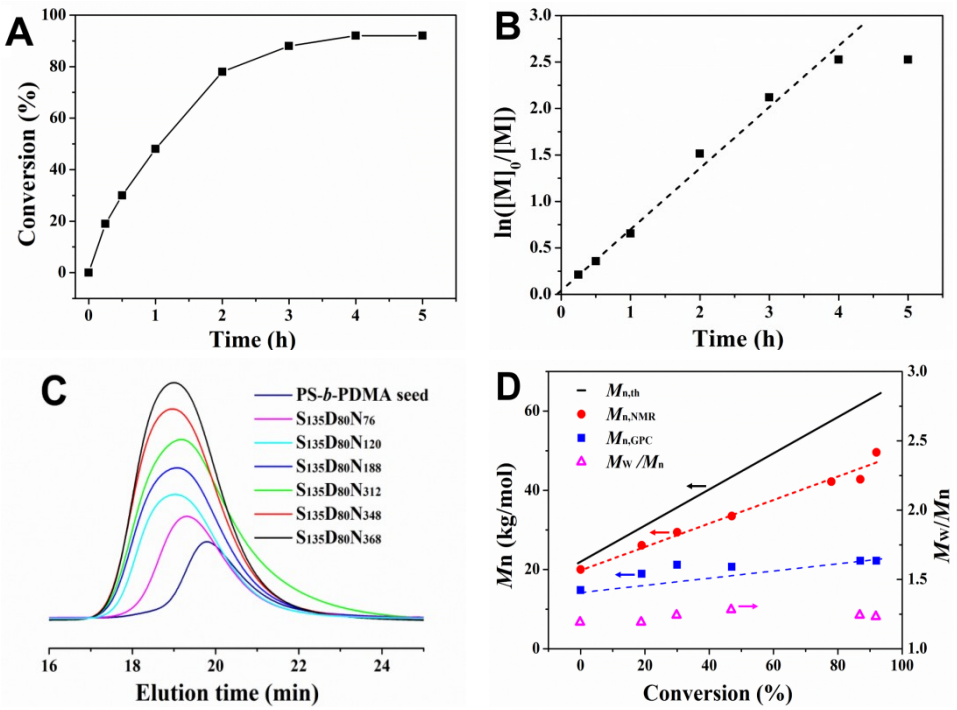

Figure 4. The monomer conversion-time plot (A) and the ln([M]$_0$/[M])-time plot (B) for the seeded RAFT polymerization of NIPAM in the presence of the seed-nanoparticles of PS$_{135}$-*b*-PDMA$_{80}$-TTC, the GPC traces (C) and the molecular weight and PDI (D) of the synthesized PS-*b*-PDMA-*b*-PNIPAM triblock terpolymers. Polymerization conditions: NIPAM (0.500 g, 4.42 mmol), the ethanol/water mixture (4.23 g, 80/20 by weight), [NIPAM]$_0$/[PS$_{135}$-*b*-PDMA$_{80}$-TTC]$_0$/[AIBN]$_0$ = 1200/3/1, 70 °C.

The kinetics of the seeded RAFT polymerization of NIPAM in the 80/20 ethanol/water mixture is summarized in Figures 4A and 4B. The seeded RAFT polymerization ran quickly and 92% monomer conversion was achieved in the initial 4 h, and the further 1 h of polymerization led to a negligible increase in the monomer conversion. The linear ln([M]$_0$/[M])-time plot in the initial 4 h is observed, and therefore the pseudo-first-order kinetics of the seeded RAFT polymerization just like a homogeneous RAFT polymerization is suggested.[42] Figure 4C shows the GPC traces of the PS-*b*-PDMA-*b*-PNIPAM triblock terpolymers synthesized at different polymerization time. Based on the GPC analysis, the molecular weight $M_{n,GPC}$ and the PDI of the PS-*b*-PDMA-*b*-PNIPAM triblock terpolymer are obtained and the values are summarized in Figure 4D. It is found that the molecular weight $M_{n,GPC}$ of the PS-*b*-PDMA-*b*-PNIPAM triblock terpolymer laggardly increases with the monomer conversion and the PDI value of the triblock terpolymer is generally below 1.3. These PS-*b*-PDMA-*b*-PNIPAM triblock terpolymers are also analyzed by ^{1}H NMR analysis (Figure 2C), and the molecular weight $M_{n,NMR}$ of the triblock terpolymer is obtained by comparing the area ratio of the characteristic chemical shift at 4.02 ppm ascribed to the PNIPAM block to that of the benzene ring ascribed to the PS block. As shown in Figure 4D, $M_{n,NMR}$ of the triblock terpolymer linearly increases with the monomer conversion. Besides, it is also found that $M_{n,NMR}$ of the triblock terpolymer is very close to the theoretical number-average molecular weight $M_{n,th}$, and whereas $M_{n,NMR}$ is larger than those of $M_{n,GPC}$ by GPC analysis. The underestimated molecular weight $M_{n,GPC}$ of the PS-*b*-PDMA-*b*-PNIPAM triblock terpolymers is due to the enhanced adsorption of the Nitrogen-containing triblock terpolymer onto the GPC columns.

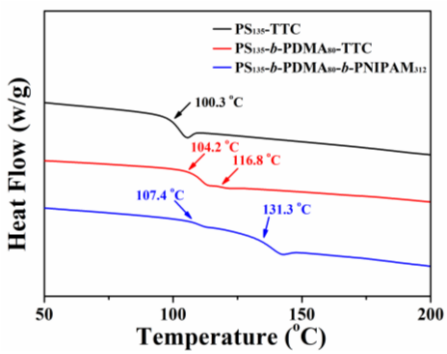

Figure 5. DSC thermograms of the homopolymer of PS$_{135}$-TTC, the diblock copolymer of PS$_{135}$-*b*-PDMA$_{80}$-TTC, and the triblock terpolymer of PS$_{135}$-*b*-PDMA$_{80}$-*b*-PNIPAM$_{312}$.

The typical PS$_{135}$-*b*-PDMA$_{80}$-*b*-PNIPAM$_{312}$ triblock terpolymer as well as the reference homopolymer of PS$_{135}$-TTC and the diblock copolymer of PS$_{135}$-*b*-PDMA$_{80}$-TTC is further characterized by DSC analysis. As shown in Figure 5, the glass transition temperature (T_g) of the reference homopolymer of PS$_{135}$-TTC is 100.3 °C, and two T_g values at 104.2 °C corresponding to the PS block and at 116.8 °C corresponding to the PDMA block are observed at the case of the PS$_{135}$-*b*-PDMA$_{80}$-TTC diblock copolymer, suggesting the PS and PDMA blocks are immiscible. As to the triblock terpolymer of PS$_{135}$-*b*-PDMA$_{80}$-*b*-PNIPAM$_{312}$, the T_g at 131.3 °C corresponding to the PNIPAM block and the T_g at 107.4 °C corresponding to the PS and/or PDMA blocks are detected. Although two T_g values but not three separate T_g values are detected herein, which is possibly due to the low fraction of the PS and/or PDMA blocks in the

triblock terpolymer, it is concluded that at least, the PNIPAM block is incompatible with the PS block. This incompatibility between the PS and PNIPAM block helps formation of the multicompartment nanoparticles of the PS_{135}-*b*-$PDMA_{80}$-*b*-$PNIPAM_{312}$ triblock terpolymer in water as discussed subsequently, when the PNIPAM block is deposited on the PS core at temperature above PTT.

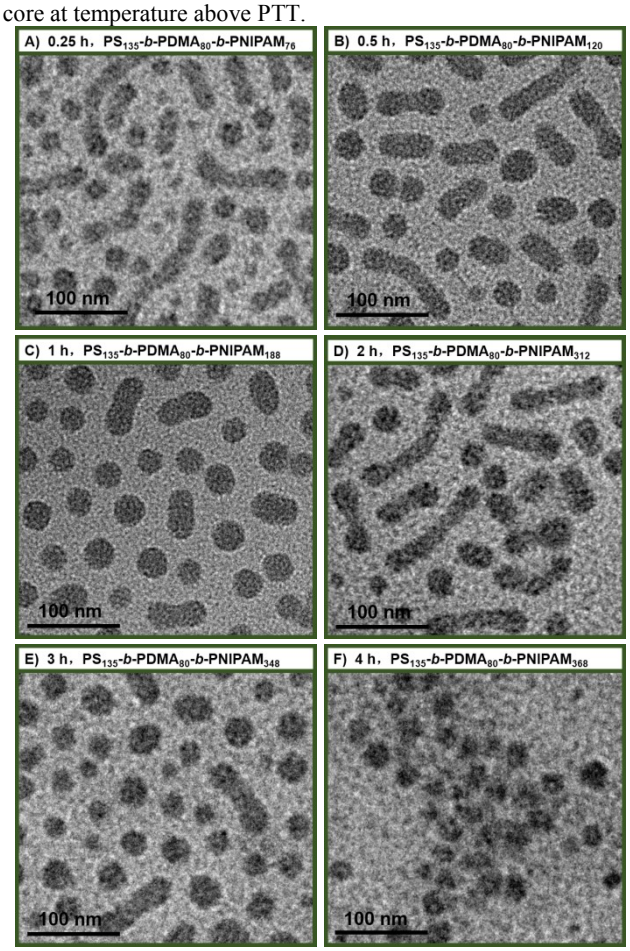

Figure 6. TEM images of the PS-*b*-PDMA-*b*-PNIPAM triblock terpolymer nano-objects prepared at the polymerization time of 0.25 h (A), 0.5 h (B), 1 h (C), 2 h (D), 3 h (E), 4 h (F).

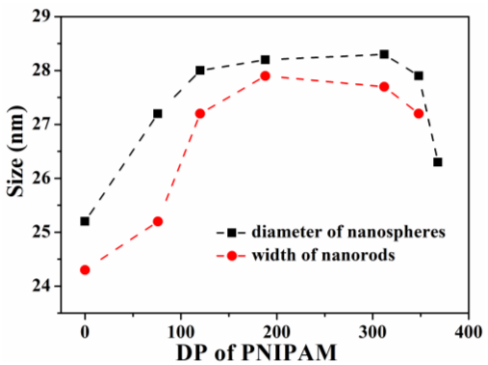

Figure 7. The evolution of the average size of the PS-*b*-PDMA-*b*-PNIPAM nano-objects with the increasing DP of the PNIPAM block.

The seeded RAFT polymerization affords the in situ synthesis of the PS-*b*-PDMA-*b*-PNIPAM nano-objects as indicated by the TEM images shown in Figures 6A-6F. At cases of the PS-*b*-PDMA-*b*-PNIPAM triblock terpolymer with the DP of the newly-formed PNIPAM block below 348, the morphology of the PS-*b*-PDMA-*b*-PNIPAM nano-objects is justly duplicated from the PS-*b*-PDMA-TTC seed-nanoparticles (Figures 6A-6E). That is, the binary mixture of the nanospheres and nanorods are in situ prepared in the seeded RAFT polymerization. When the DP of the newly-formed PNIPAM block increases to 368, the unitary nano-objects of nanospheres are formed (Figure 6F and Figure S3). The reason on the morphology transition of the PS-*b*-PDMA-*b*-PNIPAM nano-objects with the increasing DP of the PNIPAM block is discussed. As discussed elsewhere,[43] for the nano-assembly of an amphiphilic AB diblock copolymer in the block selective solvent for the B block (B-selective solvent), the AB diblock copolymer morphology depends on three contributions to the free energy of the system, namely the chain stretching in the core, the interfacial energy, and the repulsion among the corona chains. With increasing chain length of the solvophilic B block, the repulsion among corona-forming chains and the interfacial energy increase, a morphological transition following the trend of vesicles-to-rods-to-spheres occurs.[44-47] In the present study, the morphology transition of the PS-*b*-PDMA-*b*-PNIPAM nano-objects with the increasing DP of the solvophilic PNIPAM block follows the similar trend, although the ABC triblock terpolymer is involved herein. The size of the PS-*b*-PDMA-*b*-PNIPAM nano-objects is evaluated by statistical analysis of above 100 nanospheres or nanorods (Figure S2), the average diameter of the triblock terpolymer nanospheres or the width of the triblock terpolymer nanorods is obtained and the average value is summarized in Figure 7. From Figure 7, two conclusions are made. First, the width of the PS-*b*-PDMA-*b*-PNIPAM triblock terpolymer nanorods is slightly smaller or very close to the diameter of the triblock terpolymer nanospheres, which is as similarly as those in the PS-*b*-PDMA-TTC seed-nanoparticles. Second, the diameter of the triblock terpolymer nanospheres initially increases and then slightly decreases with the increasing DP of the PNIPAM block. For core-corona micelles of an amphiphilic AB diblock copolymer in the B-selective solvent, the size of core-corona micelles is related to the aggregation number (Z), the number of copolymer molecules per micelle, which depends on the polymerization degree of each block.[48] In general, the aggregation number Z for the amphiphilic AB diblock copolymer can be expressed by the equation of $Z = Z_0\left(\mathrm{DP}_A^{\alpha} \times \mathrm{DP}_B^{-\beta}\right)$,[48] in which DP_A and DP_B are the polymerization degree of the solvophobic A block and the solvophilic B block, respectively. The reason on the initial increase in the size (diameter or width) of the triblock terpolymer nano-objects with the increasing DP of the PNIPAM block is not very clear, and it is possibly ascribed to the triblock terpolymer nano-objects being kinetically frozen in the polymerization medium of the 80/20 ethanol/water mixture but not being in the thermodynamically state. With the increasing DP of the solvophilic PNIPAM block, the triblock terpolymer nano-objects are not kinetically frozen anymore, and the size of the triblock terpolymer nano-objects decreases following the trend determined by the equation of $Z = Z_0\left(\mathrm{DP}_A^{\alpha} \times \mathrm{DP}_B^{-\beta}\right)$.

3.4 Thermo-response of the triblock terpolymer nano-objects

PNIPAM is a typical thermo-responsive polymer, which shows soluble-to-insoluble phase transition in water at temperature above LCST of 32 °C.[49-51] The thermo-response of the PS-*b*-

PDMA-*b*-PNIPAM triblock terpolymer nano-objects dispersed in water was checked by turbid analysis and the results are summarized in Figure 8. The results suggest that the soluble-to-insoluble transition of the PNIPAM block in the PS_{135}-*b*-$PDMA_{80}$-*b*-$PNIPAM_{76}$ triblock terpolymer nano-objects in water occurs within a relatively narrow temperature range of 37 ± 2 °C, and the DP of the PNIPAM block seems to have no or very slight effect on the PTT of the PS-*b*-PDMA-*b*-PNIPAM nano-objects. Compared with the LCST of the PNIPAM homopolymer,[49-51] the PTT of the present PS-*b*-PDMA-*b*-PNIPAM nano-objects is a little higher. The reason is possibly due to the steric repulsion among the crowded PNIPAM chains tethered on the PS core of the triblock terpolymer nano-objects, which retards the soluble-to-insoluble transition of the tethered PNIPAM chains as discussed elsewhere.[52]

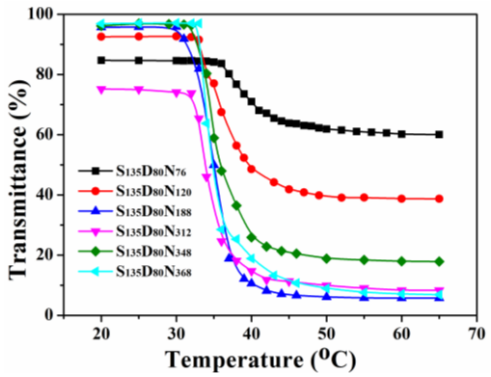

Figure 8. The transmittance versus temperature plots of the PS-*b*-PDMA-*b*-PNIPAM triblock terpolymer nano-objects in water, in which SDN represents the PS-*b*-PDMA-*b*-PNIPAM triblock terpolymer, and S represents the PS block, D represents the PDMA block and N represents the PNIPAM block. The concentration of the triblock terpolymer is 0.1 wt%.

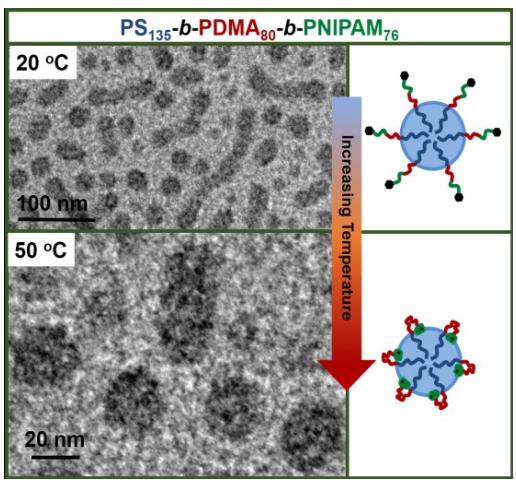

Figure 9. TEM images of PS_{135}-*b*-$PDMA_{80}$-*b*-$PNIPAM_{76}$ triblock terpolymer nano-objects in water at temperature of 20 °C (below PTT) and 50 °C (above PTT), and their schematic structures.

Since the PNIPAM block is soluble in water at temperature below PTT and it further becomes insoluble when temperature increases above PTT, therefore the morphology of the PS-*b*-PDMA-*b*-PNIPAM triblock terpolymer nano-objects at temperature below PTT and above PTT should be somewhat different. At much diluted dispersion of the PS-*b*-PDMA-*b*-PNIPAM triblock terpolymer nano-objects at temperature above PTT, it is expected that the PNIPAM chains deposit onto the PS core to form discrete micro-domains since the PNIPAM block and the PS block is incompatible as discussed above, which is confirmed by the TEM images shown in Figure 9 and Figure S4 (Note: the diluted dispersion avoids formation of bridged triblock copolymer nano-objects as discussed in ref. 53 and 54). From the high-resolution TEM images of the PS-*b*-PDMA-*b*-PNIPAM triblock terpolymer nano-objects at 50 °C above PTT, the 2~4 nm discrete nodules corresponding to the PNIPAM block on the PS core are discerned (Note: the gray domain is ascribed to the PS block, the dark-gray domain is ascribed to the PNIPAM domain, and the soluble PDMA corona is not visible in the TEM images as discussed in ref. 40), confirming the hypothesis. The formation of the PS-*b*-PDMA-*b*-PNIPAM multicompartment nano-objects at temperature above PTT of the PNIPAM block also occurs at the cases of the moderate-long and long PNIPAM block (Figure 10). Interestingly, with the increase in the DP of the PNIPAM block, the size of the PNIPAM micro-domain in the triblock terpolymer multicompartment nano-objects seems to increase slightly, *e.g.* 2~5 nm, and the discrete PNIPAM micro-domains are jointed together to form a quasi-continuous shell around the PS core as shown in Figure 10.

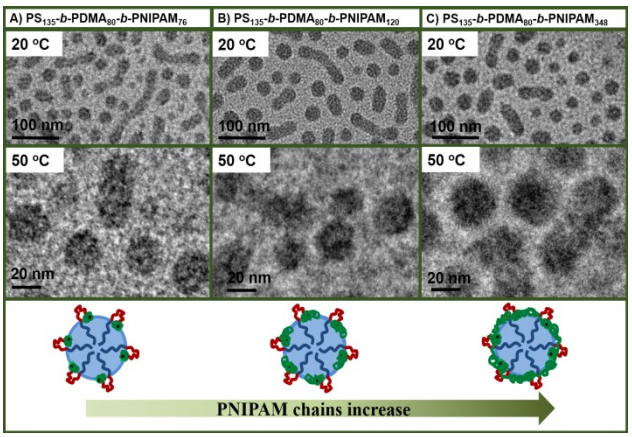

Figure 10. TEM images and the schematic structures of the triblock terpolymer nano-objects of PS_{135}-*b*-$PDMA_{80}$-*b*-$PNIPAM_{76}$ (A), PS_{135}-*b*-$PDMA_{80}$-*b*-$PNIPAM_{120}$ (B), PS_{135}-*b*-$PDMA_{80}$-*b*-$PNIPAM_{348}$ (C) in water at 20 °C below PTT and at 50 °C above PTT.

4 Conclusions

Seeded RAFT polymerization of NIPAM in the presence of the PS_{135}-*b*-$PDMA_{80}$-TTC seed-nanoparticles in the 80/20 ethanol/water mixture is performed. This seeded RAFT polymerization affords the in situ synthesis of the PS-*b*-PDMA-*b*-PNIPAM triblock terpolymer nano-objects with the polymer concentration up to 15 wt%. The molecular weight of the PS-*b*-PDMA-*b*-PNIPAM triblock terpolymer linearly increases with the monomer conversion of NIPAM during the seeded RAFT polymerization and the PDI value of the triblock terpolymer is generally below 1.3. The morphology of the PS-*b*-PDMA-*b*-PNIPAM triblock terpolymer nano-objects is justly duplicated from the PS-*b*-PDMA-TTC diblock copolymer seed-nanoparticles, which are the binary mixture of nanospheres and nanorods, when the DP of the PNIPAM block is low or moderately large. When the DP of the PNIPAM block is

relatively large, the unitary morphology of the PS-*b*-PDMA-*b*-PNIPAM triblock terpolymer nanospheres is formed. The size of the PS-*b*-PDMA-*b*-PNIPAM triblock terpolymer nano-objects initially slightly increases and then decreases with the monomer conversion during the seeded RAFT polymerization. In water, the PS-*b*-PDMA-*b*-PNIPAM triblock terpolymer nano-objects are temperature-sensitive due to the PNIPAM block, and the PTT shows no or very slight dependence on the DP of the PNIPAM block. At temperature above PTT, the PNIPAM chains deposit onto the PS core, and therefore the multicompartment triblock terpolymer nano-objects containing a microphase separated PS/PNIPAM core and a PDMA corona are formed. Our finds are anticipated to be useful to prepare concentrated ABC triblock terpolymer nano-objects, especially useful in the preparation of the multicompartment triblock terpolymer nano-objects.

ACKNOWLEDGMENTS

The financial support by National Science Foundation of China (№. 21274066), NFFTBS (№. J1103306), and PCSIRT (IRT1257) is gratefully acknowledged.

Notes and references

Key Laboratory of Functional Polymer Materials of the Ministry of Education, Collaborative Innovation Center of Chemical Science and Engineering (Tianjin), Institute of Polymer Chemistry, Nankai University, Tianjin 300071, China.

**To whom correspondence should be addressed. E-mail: wqzhang@nankai.edu.cn, Tel: 86-22-23509794, Fax: 86-22-23503510.*

† Electronic Supplementary Information (ESI) available: Text showing the chemical structure of ECT, and Figures S1 and S2 showing the TEM images of the seed-nanoparticles of PS_{135}-*b*-$PDMA_{80}$-TTC and the PS_{135}-*b*-$PDMA_{80}$-*b*-$PNIPAM_{368}$ triblock terpolymer nanospheres. Details of any supplementary information available should be included here. See DOI: 10.1039/b000000x/

1 I. W. Wyman and G. Liu, *Polymer,* 2013, **54,** 1950-1978.
2 A. H. Gröschel, A.Walther, T. I. Löbling, J. Schmelz, A. Hanisch, H. Schmalz and A. H. E. Müller, *J. Am. Chem. Soc.,* 2012, **134,** 13850-13860.
3 T. Jiang, L. Wang, S. Lin, J. Lin and Y. Li, *Langmuir,* 2011, **27,** 6440-6448.
4 K. Skrabania, H. Berlepsch, C. Böttcher and A. Laschewsky, *Macromolecules,* 2010, **43,** 271-281.
5 J. -N. Marsat, M. Heydenreich, E. Kleinpeter, H. Berlepsch, C. Böttcher and A. Laschewsky, *Macromolecules,* 2011, **44,** 2092-2105.
6 Y. Zhang, W. Lin, R. Jing and J. Huang, *J. Phys. Chem. B,* 2008, **112,** 16455-16460.
7 M. J. Barthel, U. Mansfeld, S. Hoeppener, J. A. Czaplewska, F. H. Schacher and U. S. Schubert, *Soft Matter,* 2013, **9,** 3509-3520.
8 G. Njikang, D. Han, J. Wang and G. Liu, *Macromolecules,* 2008, **41,** 9727-9735.
9 C. Zhou, M. A. Hillmyer and T. P. Lodge, *J. Am. Chem. Soc.,* 2012, **134,** 10365-10368.
10 V. Schmidt, R. Borsali and C. Giacomelli, *Langmuir,* 2009, **25,** 13361-13367.
11 Y. Cai, K. B. Aubrecht and R. B. Grubbs, *J. Am. Chem. Soc.,* 2011, **133,** 1058-1065.
12 E. Betthausen, M. Drechsler, M. Förtsch, F. H. Schacher and A. H. E. Müller, *Soft Matter,* 2011, **7,** 8880-8891.
13 N. Willet, J.-F. Gohy, L. Lei, M. Heinrich, L. Auvray, S. Varshney, R. Jérôme and B. Leyh, *Angew. Chem. Int. Ed.,* 2007, **46,** 7988-7992.
14 W. Zhang, X Jiang, Z. He, D. Xiong, P. Zheng, Y. An and L. Shi, *Polymer,* 2006, **47,** 8203-8209.
15 H. Cui, Z. Chen, K. L. Wooley and D. J. Pochan, *Soft Matter,* 2009, **5,** 1269-1278.
16 C. Luo, Y. Liu and Z. Li, *Soft Matter,* 2012, **8,** 2618-2626.
17 J. Hu, G. Njikang and G. Liu, *Macromolecules,* 2008, **41,** 7993-7999.
18 S. Yu, T. Azzam, I. Rouiller and A. Eisenberg, *J. Am. Chem. Soc.,* 2009, **131,** 10557-10566.
19 A. Sundararaman, T. Stephan and R. B. Grubbs, *J. Am. Chem. Soc.,* 2008, **130,** 12264-12265.
20 C. Zhou, M. A. Hillmyer and T. P. Lodge, *Macromolecules,* 2011, **44,** 1635-1641.
21 D. Xie, X. Ye, Y. Ding, G. Zhang, N. Zhao, K. Wu, Y. Cao and X. X. Zhu, *Macromolecules,* 2009, **42,** 2715-2720.
22 C. L. McCormick, B. S. Sumerlin, B. S. Lokitz and J. E. Stempka, *Soft Matter,* 2008, **4,** 1760-1773.
23 C. Ott, R. Hoogenboom, S. Hoeppener, D. Wouters, J.-F. Gohy and U. S. Schubert, *Soft Matter,* 2009, **5,** 84-91.
24 K. Yamauchi, H. Hasegawa, T. Hashimoto, N. Köhler and K. Knoll, *Polymer,* 2002, **43,** 3563-3570.
25 R.-S. Lee, W.-H. Chen and Y.-T. Huang, *Polymer,* 2010, **51,** 5942-5951.
26 A. J. Convertine, B. S. Lokitz, Y. Vasileva, L. J. Myrick, C. W. Scales, A. B. Lowe and C. L. McCormick, *Macromolecules,* 2006, **39,** 1724-1730.
27 S. Kessel, N. P. Truong, Z. Jia and M. J. Monteiro, *J. Polym. Sci. Part A: Polym. Chem.,* 2012, **50,** 4879-4887.
28 A. B. Lowe, M. Torres and R. Wang, *J. Polym. Sci. Part A: Polym. Chem.,* 2007, **45,** 5864-5871.
29 J. Mao, S. Bo and X. Ji, *Langmuir*, 2011, **27,** 7385-7391.
30 H. Wei, S. Perrier, S. Dehn, R. Ravarian and F. Dehghani, *Soft Matter,* 2012, **8,** 9526-9528.
31 Y. Zheng, L. Wang, R. Yu and S. Zheng, *Macromol. Chem. Phys.,* 2012, **213,** 458-469.
32 B. H. Lessard, E. J. Y. Ling and M. Marić, *Macromolecules,* 2012, **45,** 1879-1891.
33 X. Xu, J. D. Flores and C. L. McCormick, *Macromolecules,* 2011, **44,** 1327-1334.
34 Y. Li, B. S. Lokitz and C. L. McCormick, *Macromolecules,* 2006, **39,** 81-89.
35 F. Huo, C. Gao, M. Dan, X. Xiao, Y. Su and W. Zhang, *Polym. Chem.,* 2014, **5,** 2736-2746.
36 M. Dan, F. Huo, X. Xiao, Y. Su and W. Zhang, *Macromolecules,* 2014, **47,** 1360-1370.
37 X. Xiao, S. He, M. Dan, F. Huo and W. Zhang, *Chem. Commun.*, 2014, **50**, 3969-3972.
38 B. Charleux, G. Delaittre, J. Rieger and F. D'Agosto, *Macromolecules*, 2012, 45, 6753-6765.
39 G. Moad, Y. K. Chong, A. Postma, E. Rizzardo and S. H. Tang, *Polymer,* 2005, 46, 8458-8468.
40 F. Huo, S. Li, Q. Li, Y. Qu and W. Zhang, *Macromolecules,* 2014, **47,** 2340-2349.
41 H. D. Brouwer, M. A. J. Schellekens, B. Klumperman, M. J. Monteiro and A. L. German, *J. Polym. Sci. Part A: Polym. Chem.,* 2000, **38,** 3596-3603.
42 A. B. Lowe and C. L. McCormick, *Prog. Polym. Sci.,* 2007, **32,** 283-351.
43 X. Li, P. Tang, F. Qiu, H. Zhang and Y. Yang, *J. Phys. Chem. B*, 2006, **110,** 2024-2030.
44 S. Sugihara, A. Blanazs, S. P. Armes, A. J. Ryan and A. L. Lewis, *J. Am. Chem. Soc.,* 2011, **133,** 15707-15713.
45 L. P. D. Ratcliffe, A. J. Ryan and S. P. Armes, *Macromolecules,* 2013, **46,** 769-777.
46 A. Blanazs, J. Madsen, G. Battaglia, A. J. Ryan and S. P. Armes, *J. Am. Chem. Soc.,* 2011, **133,** 16581-16587.
47 W.-D. He, X.-L. Sun, W. -M. Wan and C.-Y. Pan, *Macromolecules,* 2011, **44,** 3358-3365.
48 S. I. Yoo, B.-H. Sohn, W.-C. Zin, J. C. Jung and C. Park, *Macromolecules,* 2007, **40,** 8323-8328.
49 R. Plummer, D. J. T. Hill and A. K. Whittaker, *Macromolecules,* 2006, **39,** 8379-8388.
50 J. Xu, J. Ye and S. Liu, *Macromolecules,* 2007, **40,** 9103-9110.

51 M. E. Alf, T. A. Hatton and K. K. Gleason, *Polymer,* 2011, **52,** 4429-4434.
52 C. Yang, J. N. Kizhakkedathu, D. E. Brooks, F. Jin and C. Wu, *J. Phys. Chem. B,* 2004, **108,** 18479-18484.
53 R. R. Taribagil, M. A. Hillmyer and T. P. Lodge, *Macromolecules,* 2009, **42,** 1796-1800.
54 J. Madsen and S. P. Armes, *Soft Matter,* 2012, **8,** 592-605.

For Table of Contents use only

In situ synthesis of thermo-responsive ABC triblock terpolymer nano-objects by seeded RAFT polymerization

Yaqing Qu, Fei Huo, Quanlong Li, Xin He, Shentong Li, and Wangqing Zhang*

Key Laboratory of Functional Polymer Materials of the Ministry of Education, Collaborative Innovation Center of Chemical Science and Engineering (Tianjin), Institute of Polymer Chemistry, Nankai University, Tianjin 300071, China.

*To whom correspondence should be addressed. E-mail: wqzhang@nankai.edu.cn, Tel: 86-22-23509794, Fax: 86-22-23503510.

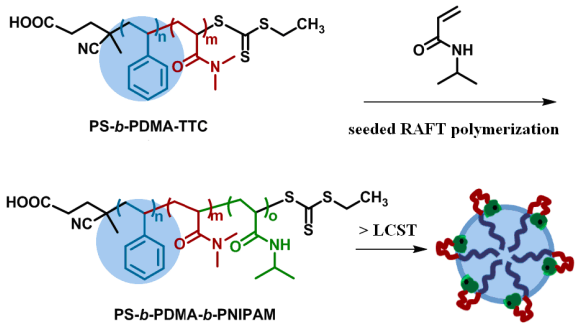

Synthesis of thermo-responsive ABC triblock terpolymer nano-objects by seeded RAFT polymerization is achieved. At temperature above LCST, the triblock terpolymer nano-objects convert into multicompartment nanoparticles.